Amino Acids (2005) 29: 389–404
DOI 10.1007/s00726-005-0203-z

Amino Acids
Printed in Austria

Catabolism of native and oxidized low density lipoproteins: *in vivo* insights from small animal positron emission tomography studies*

J. Pietzsch, R. Bergmann, F. Wuest, B. Pawelke, C. Hultsch, and **J. van den Hoff**

Positron Emission Tomography Center, Institute of Bioinorganic and Radiopharmaceutical Chemistry, Research Center Rossendorf, Dresden, Germany

Received November 1, 2004
Accepted February 7, 2005
Published online July 15, 2005;

Summary. The human organism is exposed to numerous processes that generate reactive oxygen species (ROS). ROS may directly or indirectly cause oxidative modification and damage of proteins. Protein oxidation is regarded as a crucial event in the pathogenesis of various diseases ranging from rheumatoid arthritis to Alzheimer's disease and atherosclerosis. As a representative example, oxidation of low density lipoprotein (LDL) is regarded as a crucial event in atherogenesis. Data concerning the role of circulating oxidized LDL (oxLDL) in the development and outcome of diseases are scarce. One reason for this is the shortage of methods for direct assessment of the metabolic fate of circulating oxLDL *in vivo*. We present an improved methodology based on the radiolabelling of apoB-100 of native LDL (nLDL) and oxLDL, respectively, with the positron emitter fluorine-18 (^{18}F) by conjugation with *N*-succinimidyl-4-[^{18}F]fluorobenzoate ([^{18}F]SFB). Radiolabelling of both nLDL and oxLDL using [^{18}F]SFB causes neither additional oxidative structural modifications of LDL lipids and proteins nor alteration of their biological activity and functionality, respectively, *in vitro*. The method was further evaluated with respect to the radiopharmacological properties of both [^{18}F]fluorobenzoylated nLDL and oxLDL by biodistribution studies in male Wistar rats. The metabolic fate of [^{18}F]fluorobenzoylated nLDL and oxLDL in rats *in vivo* was further delineated by dynamic positron emission tomography (PET) using a dedicated small animal tomograph (spatial resolution of 2 mm). From this study we conclude that the use of [^{18}F]FB-labelled LDL particles is an attractive alternative to, e.g., LDL iodination methods, and is of value to characterize and to discriminate the kinetics and the metabolic fate of nLDL and oxLDL in small animals *in vivo*.

Keywords: Low density lipoprotein – Bolton-Hunter type reagent – LDL radiolabelling – Protein oxidation – Small animal positron emission tomography.

1 Introduction

It is well known that oxidative modifications in the structure of proteins are implicated either in the etiology, progression, or manifestation of various inflammatory, neurodegenerative, and metabolic diseases ranging from rheumatoid arthritis to Alzheimer's disease and atherosclerosis. In the living organism the steady-state level of oxidized protein reflects the balance between the rate of protein oxidation by reactive oxygen species (ROS) on the one hand and the rate of oxidized protein degradation on the other (Stadtman and Berlett, 1998). This balance is a complex function of ROS-generating systems, enzymatic and non-enzymatic antioxidant defense systems, and proteases that degrade oxidized proteins. Elevated levels and accumulation of oxidized proteins in several body compartments can either reflect an accelerated increase in the rate of ROS generation, a decrease in proteolytic activities, or simultaneous changes in all of these factors (Stadtman and Berlett, 1998; Stadtman and Levine, 2003). This endorses the concept of 'oxidative stress' originally established 20 years ago (Sies, 1985).

Eventually, oxidative modification of proteins can interfere with critical cellular functions and affect enzyme function and cellular signalling. In this line, apolipoprotein (apo) B-100, the major protein of human low density lipoproteins (LDL), is of particular pathophysiological importance. Oxidative modification of apoB-100 by ROS is widely regarded as a crucial event in the atherogenic process – the ''oxidative modification hypothesis of

*A part of this report has been presented at the 74th European Atherosclerosis Society Congress, Seville, Spain, 17–20 April 2004, and has been published in abstract form: Pietzsch J, Bergmann R, Wuest F, Pawelke B, van den Hoff J (2004) Assessment of metabolism of native and oxidized low density lipoprotein *in vivo*: insights from animal positron emission tomography (PET) studies. Atherosclerosis 5 [Suppl 1]: 143–144.

atherosclerosis'' (Ross, 1999; Stocker and Keaney, 2004). For apoB-100 these modifications, e.g., covalent binding of lipid peroxidation and glycoxidation products, respectively, or, probably much more important, direct oxidation of amino acid side chain residues, are thought to strikingly change its structural and functional properties that finally result in the formation of new epitopes. The latter are specifically recognized by scavenger receptors, followed by an excessive uptake and accumulation of LDL particles in macrophages, vascular smooth muscle cells, and endothelial cells in an unregulated fashion that can lead to foam cell formation (Dhaliwal and Steinbrecher, 1999; Heinecke, 2002). The presence of foam cells in the vascular wall is considered to be the first morphological substrate of atherosclerosis (Ross, 1999). Recently, direct oxidation of LDL apoB-100 has been measured in LDL particles recovered from human aortic vascular lesions (Pietzsch and Bergmann, 2003; Pietzsch et al., 2004a). Moreover, direct oxidation of LDL apoB-100 has been measured in circulating LDL *in vivo* in conditions which are accompanied by rapidly developing atherosclerosis including hypercholesterolemia, impaired glucose tolerance, diabetes, and rheumatoid arthritis (Pietzsch et al., 2000; Pietzsch et al., 2004b; Julius and Pietzsch, in press).

Despite the evidence from experimental and clinical studies concerning the importance of oxidized LDL (oxLDL), the role of circulating oxLDL particles in the development of atherosclerosis *in vivo* is still a matter of debate. Furthermore, the diagnostic significance of circulating oxLDL in blood in several human pathologies is poorly understood. One reason for this is the lack of sensitive and specific radiolabelling methods, which would allow direct assessment of intravascular transfer and catabolism of oxLDL *in vivo*.

Radiolabelling of whole lipoproteins or individual apolipoproteins has been established as an essential tool for determination of the kinetics of lipoprotein metabolism in humans and animals *in vivo* (Hugh et al., 1996; Burnett and Barrett, 2002). Various radionuclides have been used to label LDL. However, investigations to evaluate localization, clearance, and biological effects of modified LDL, e.g., acetylated LDL and oxidized LDL, respectively, have used extensively iodine-125 and iodine-131 (Sasaki and Cottam, 1982; Raymond et al., 1986; van Berkel et al., 1991; Ottnad et al., 1992; Chang et al., 1993; De Rijke et al., 1994; Bjornheden et al., 1998; Shaish et al., 2001). The value of radiolabelled lipoproteins as tracers for biological studies is based on the assumption that their biological properties are not altered by the labelling procedure or by the radioisotope itself. Recently, several authors clearly demonstrated that most commonly used radioiodination methods such as iodogen, chloramine-T, or iodine monochloride lead to oxidative modification of both the lipid and the protein moiety of LDL, affecting their lipid and apolipoprotein integrity, interaction with LDL receptors or scavenger receptors, and *in vivo* clearance (Khouw et al., 1993; Romero et al., 2001; Sobal et al., 2004). As explicitly stated in these studies, it has to be realized that radioiodinated LDL no longer reflect the native LDL (nLDL) particle or, when obtained from *in vitro* oxidation experiments, the initially characterized modified LDL particle (Khouw et al., 1993; Romero et al., 2001; Sobal et al., 2004). Consequently, the use of radioiodinated LDL labelled via direct iodination has striking disadvantages. Particularly, it does not allow to differentiate kinetics and behaviour of native and oxidized LDL *in vivo* (Sobal et al., 2004).

Very recently, we proposed a novel methodology for no-carrier-added (*n.c.a.*) labelling of LDL with the positron emitter fluorine-18 (^{18}F) using the Bolton-Hunter-type reagent *N*-succinimidyl-[4-^{18}F]fluorobenzoate ([^{18}F]SFB) (Pietzsch et al., 2004c). We have shown that radiolabelling of both nLDL and oxLDL using [^{18}F]SFB caused neither additional oxidative structural modifications of LDL lipids and proteins nor alteration of their biological activity and functionality *in vitro*, respectively (Pietzsch et al., 2004c). In this study we extend our earlier observations by investigation of the *in vivo* catabolism of both [^{18}F]FB-nLDL and [^{18}F]FB-oxLDL in biodistribution experiments and dynamic small animal PET studies in male Wistar rats. Results suggest that the use of radiolabelling of both nLDL and oxLDL using [^{18}F]SFB is of value to characterize and differentiate the metabolic fate of native and oxidized LDL *in vivo*.

2 Materials and methods

2.1 LDL isolation and oxidation

Native LDL (density 1.006–1.063 g/mL) were isolated from the plasma of healthy, normolipidemic, normoglycemic male volunteers by very fast ultracentrifugation (VFU) as previously described (Pietzsch et al., 2004c). The isolated LDL were free of albumin and other contaminating plasma proteins (Pietzsch et al., 1995). LDL apoB-100 was measured by immunoelectrophoresis using 'ready-to-use' agarose gels (Sebia, Issy-les-Moulineaux, France). LDL cholesterol content was assayed enzymatically using CHOD-PAP test kits (Roche, Mannheim, Germany). Immediately before oxidation of LDL, EDTA, and salt from the density gradient were removed using a size exclusion column (Econo-Pac 10DG, Bio-Rad) and phosphate-buffered saline (PBS, 10 mM sodium phosphate, 150 mM sodium chloride, pH 7.2) as the eluent. For oxidation, aliquots of native LDL (600 μg apoB-100/mL, equal to 1.2 μM LDL) were subjected to a well characterized iron-catalyzed oxidation system containing 10 μM

bovine hemin chloride and 100 μM H_2O_2 at 37°C for 40 hours in the dark (Pietzsch, 2000; Pietzsch and Bergmann, 2004).

2.2 Measurement of parameters of apoB-100 oxidation

Before to and after the radiolabelling procedure, the extent of LDL apoB-100 oxidation was evaluated by determination of relative electrophoretic mobility (REM), generation of autofluorescence products at 360/430 nm, total carbonyl group content, and by determining the formation of highly specific products of oxidation of positively charged protein amino acid residues, γ-glutamyl semialdehyde and α-aminoadipic semialdehyde, which by reduction form 5-hydroxy-2-aminovaleric acid (HAVA) and 6-hydroxy-2-aminocaproic acid (HACA), respectively (Kopprasch et al., 1998; Pietzsch, 2000; Pietzsch et al., 2004c). The content of total carbonyl groups, HAVA, and HACA in LDL is expressed as mol/mol apoB-100.

2.3 Radiolabelling of nLDL and oxLDL with [^{18}F]SFB

Synthesis of [^{18}F]SFB was performed as described previously (Wuest et al., 2003). No-carrier-added (*n.c.a.*) [^{18}F]SFB was obtained in decay-corrected radiochemical yields of 44–53% and radiochemical purity of >95%, respectively, within 40 min after end of bombardment (Wuest et al., 2003). Both nLDL and oxLDL were radiolabelled with [^{18}F]SFB as follows (*cf.* Pietzsch et al., 2004c). [^{18}F]SFB was first evaporated under a stream of nitrogen. 1 mL LDL (0.12 mg apoB-100/mL) in phosphate-buffered saline (PBS; 10 mM sodium phosphate, 150 mM sodium chloride, pH 7.2) was added to dried [^{18}F]SFB. The reaction mixture was incubated for 20 min at room temperature. To remove unreacted [^{18}F]SFB and radioactive by-products, particularly, [^{18}F]fluorobenzoic acid formed by competing hydrolysis, the complete solution (1 mL) was eluted over a size exclusion column (Econo-Pac 10DG containing Bio-Gel P6, 10 mL bed volume; Bio-Rad) with a flow rate of 2.5 mL/min using PBS as the eluent. The purification was followed by measurement of [^{18}F]-radioactivity, apoB-100 concentration, and total cholesterol concentration in each fraction collected (0.25 mL fraction size). Furthermore, aliquots of both the reaction mixture and the fractions corresponding to [^{18}F]fluorobenzoylated LDL ([^{18}F]FB-LDL) were subjected to SDS-PAGE as reported elsewhere (*cf.* Pietzsch et al., 2004c). Finally, the fractions containing purified [^{18}F]FB-LDL (total product volume ranged between 0.5 and 1 mL) were sterilized by filtration over a Millipore GS filter.

2.4 Cell culture and lipoprotein uptake

The perpetuation of the biological activity in terms of specific cellular binding and uptake of both radiolabelled [^{18}F]FB-nLDL and [^{18}F]FB-oxLDL was assessed in human hepatocyte carcinoma cell line HepG2 and human monocyte cell line THP-1, respectively (*cf.* Pietzsch et al., 2004c).

2.5 In vivo stability and biodistribution studies

All animal experiments were carried out with male Wistar rats (Kyoto-Wistar strain; aged 6 weeks; 160–170 g) according to the guidelines of the German Regulations for Animal Welfare. The protocol was approved by the local Ethical Committee for Animal Experiments. Animals were kept under a 12 h light-dark cycle and fed with commercial animal diet and water *ad libitum*.

For biodistribution studies, the animals were injected into the tail vein under light ether anaesthesia. The injection volume of either [^{18}F]FB-LDL or [^{18}F]FB-oxLDL (0.8–1.2 MBq; radiochemical purity 96%; PBS, pH 7.2) was 0.5 mL. Biodistribution was determined in groups of eight rats sacrificed 5 and 60 min post injection (*p.i.*), respectively, by heart puncture under ether anaesthesia. Organs and tissues of interest were rapidly excised, weighed, and the radioactivity was determined (Cobra II gamma counter, Canberra-Packard, Meriden, CT, USA). The accumulated radioactivity in organs and tissues was calculated as the percentage of the injected dose per gram tissue (% ID/g tissue).

For metabolite analysis, animals were anesthetized with urethane (1.3 g/kg body weight) and catheters were placed into both the right external jugular vein and the right common carotid artery. A volume of 0.5 mL of either [^{18}F]FB-LDL or [^{18}F]FB-oxLDL (10 MBq; radiochemical purity 96%; PBS, pH 7.2) was injected in the vein. At 5, 10, 30, and 60 min after injection blood samples (0.3 mL) were taken from the arteria. The depleted blood volume was compensated for by injection of saline. 60 min after injection the animals were sacrificed and urine samples were taken (0.5 mL). Blood samples were centrifuged at 4°C (2000 × g for 10 min). Both plasma and urine samples were deproteinated with the twofold volume of 45% methanol containing 5% TFA.

The plasma and urine samples were analysed by HPLC. The HPLC system (HP1100, Agilent Technologies, Waldbronn, Germany) was equipped with a guard-column (ZORBAX 300SB-C18, 4.6 × 12.5 mm, 5 μm), a semi-preparative column (ZORBAX 300SB-C18, 9.4 × 250 mm, 5 μm), a variable-wavelength UV detector and a radio-chromatography detector (Canberra-Packard, Meriden, CT, USA). Typically, 50–200 μL (10–20 kBq) plasma or urine were injected and compounds were separated using gradient conditions at 40°C and a flow rate of 2 mL/min. Solvent A comprised of acetonitrile with 0.04% TFA, solvent B comprised of water with 0.05% TFA. The gradient steps were: 0–10 min 10% to 20% A, 10–15 min 20% to 80% A, 15–19 min 80% A. For UV-detection the wavelength of 214 nm was used. The reference compounds *N*-4-[^{18}F]fluorobenzoyl-glycine (4-[^{18}F]fluorohippurate), 4-[^{18}F]fluorobenzoic acid, and [^{18}F]SFB, eluted on this system with retention times of 14.4, 18.9, and 19.7 min.

2.6 Dynamic small animal PET studies

Dynamic small animal PET studies were performed with a dedicated PET scanner for small animals (microPET P4, CTI Concorde Microsystems, Knoxville, TN, USA). The scanner has a field-of-view (FOV) of 8 cm axially by 22 cm transaxially and operates in 3-dimensional list mode. The raw data were sorted into three-dimensional sinogram data and converted to two-dimensional format by Fourier rebinning (FORE). Iterative image reconstruction was performed using two-dimensional ordered subsets expectation maximization (OSEM) (Defrise et al., 1997; Liu et al., 2001). Image reconstruction was carried out with attenuation correction. Corrections were applied for variability in line of response detection efficiency (normalization) and random coincidences. The spatial resolution obtained with this reconstruction ranged from 2.2 to 2.3 mm. No correction for recovery and partial volume effects was applied. The scanner was cross-calibrated with an activimeter for ^{18}F. For imaging studies, animals were anesthetized with urethane (1.3 g/kg body weight) and catheters were placed into the right external jugular vein or, alternatively, into the femoral vein. The animals under urethane anesthesia were then positioned and immobilized supine with their medial axis parallel to the axial axis of the scanner with thorax and abdominal region (organs of interest: heart, liver, kidneys, bladder) in the center of FOV. For the purpose of photon attenuation correction, a transmission scan was carried out for 18 min before tracer administration. The radiotracers were then administered as a 0.5 mL bolus via the catheters within 15 seconds. In a typical experiment, either [^{18}F]FB-LDL or [^{18}F]FB-oxLDL (10 MBq; radiochemical purity 96%; PBS, pH 7.2) was injected. Simultaneously with tracer injection, dynamic PET scanning was started for 60–120 min using the following time intervals (frames) for sinogram generation: 12 × 10 s, 6 × 30 s, 5 × 300 s, 3 × 600 s, and 4 × 900 s. Images were analysed by assigning 3-dimensional regions-of-interest (ROI) over the heart region (majorily representing the cardiac blood pool), the liver and the kidneys using the ROIFinder software package developed by Poetzsch and colleagues (Poetzsch et al., 2003). From these ROIs time-activity-curves (TACs) representing the total ^{18}F-radioactivity concentration in a defined volume and expressed as radioactivity concentration, percent of maximum were

obtained from the PET images in each rat. At the end of the PET studies the rats were sacrificed by intravenous application of KCl and whole-body static PET scans were performed afterwards.

3 Results

3.1 Radiolabelling of LDL

Both native LDL (nLDL) and oxidized LDL (oxLDL) were radiolabelled with the positron emitter ^{18}F by conjugation with [^{18}F]SFB (Pietzsch et al., 2004c). Figure 1 shows the proposed reaction scheme. The maximum degree of binding was achieved after 20 min of incubation at room temperature using 0.12 mg apoB-100/mL in phosphate-buffered saline (10 mM sodium phosphate, 150 mM sodium chloride) at pH 7.2. The coupling reaction of both nLDL and oxLDL with *n.c.a.* [^{18}F]SFB resulted in radiolabelled LDL particles that were completely separated by gel filtration from unreacted [^{18}F]SFB and radioactive by-products, e.g., [^{18}F]fluorobenzoic acid (Fig. 2). In agreement with former results, in purified radiolabelled LDL particles more than 96% of total ^{18}F radioactivity (decay-corrected) could be recovered in the intact apoB-100 molecule (Pietzsch et al., 2004c) (Fig. 3). Of note, no fragmentation or aggregation of LDL apoB-100 occurred during the hemin-catalyzed oxidation or the radiolabelling procedure (Fig. 3). Only trace amounts ($<1\%$ in total) of other radiolabelled apolipoproteins, particularly, apoE were found. A maximum of 2% of LDL-bound ^{18}F radioactivity was extractable with an ice-cold chloroform:methanol mixture (2:1, v/v) and found to be either non-covalently associated with the lipid layer or bound to phospholipids containing primary amino groups. The total radiochemical yield (corrected for decay, related to [^{18}F]SFB) was $32 \pm 11\%$ for [^{18}F]FB-nLDL and $28 \pm 9\%$ for [^{18}F]FB-oxLDL, respectively.

In a typical experiment, 800 MBq of [^{18}F]SFB could be converted into 180 MBq (30%, decay-corrected) of

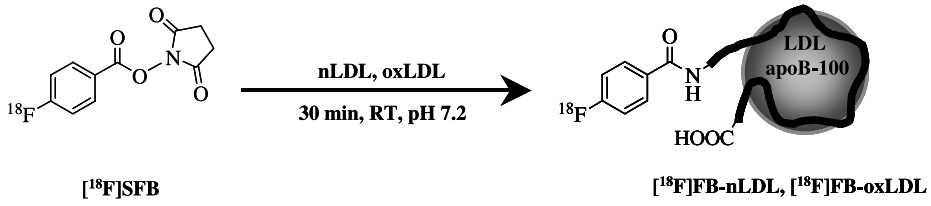

Fig. 1. Proposed reaction scheme of selective [^{18}F]fluorobenzoylation of LDL apoB-100 at its chemically accessible glutamate amino-terminal residue at pH 7.2

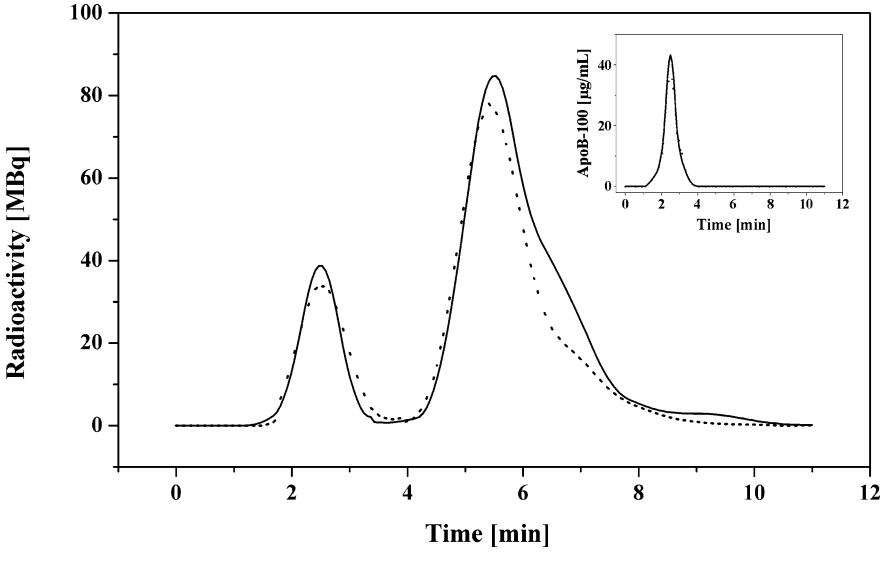

Fig. 2. Representative elution patterns of [^{18}F]FB-nLDL (solid line) and [^{18}F]FB-oxLDL (dotted line) on a DG 10 size exclusion chromatography column. LDL were radiolabelled and chromatographed as described in the *Methods* section. The insert shows co-elution of apoB-100 content of [^{18}F]FB-nLDL (solid line) and [^{18}F]FB-oxLDL (dotted line), respectively

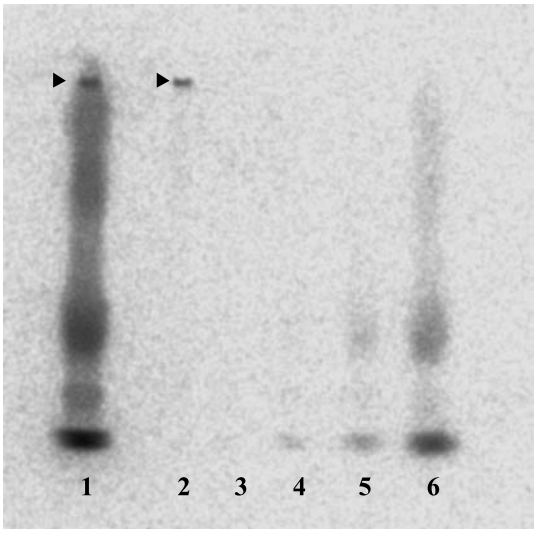

Fig. 3. Representative SDS polyacrylamide gel electrophoresis pattern of a complete separation of [^{18}F]FB-oxLDL. The figure shows radioactivity distribution as determined by radioluminography using a BAS 5000 scanner (FUJIX, Tokyo, Japan). Lane 1 is the reaction mixture, lanes 2 to 6 represent individual fractions obtained from DG 10 size exclusion chromatography column. Arrows indicate the apoB-100 band

[^{18}F]fluorobenzoylated LDL within 45 min, including size-exclusion chromatography purification. The purified [^{18}F]fluorobenzoylated LDL had an effective specific radioactivity in the range of 200–500 GBq/μmol for both [^{18}F]FB-nLDL and [^{18}F]FB-oxLDL (each related to apoB-100; M_r 516.000, without carbohydrate content) at the time of *in vitro* and *in vivo* studies. Furthermore, both [^{18}F]FB-nLDL and [^{18}F]FB-oxLDL showed high *in vitro* stability at several time points (30 min, 2 h, and 4 h after radiolabelling) using PBS (pH 6.5 to 7.5) and blood plasma as the solvent at 37°C. At each time point after labelling more than 96% of total [^{18}F]-radioactivity (decay-corrected) could be recovered in the intact apoB-100 molecule (*cf.* Pietzsch et al., 2004c).

3.2 In vitro investigations

Non-specific as well as specific parameters of LDL apoB-100 oxidation were determined in nLDL and oxLDL before and after the radiolabelling procedure (Table 1). As expected, exposure of native LDL particles to hemin (Fe^{3+}-protoporphyrin IX) as pro-oxidant lead to the formation of oxidized LDL particles accompanied by a marked increase of all oxidation parameters measured. The levels of these parameters found in this experiment correspond well to data published elsewhere (Pietzsch, 2000; Pietzsch and Bergmann, 2004; Sobal et al., 2004).

Table 1. Parameters of protein oxidation prior to and after radiolabelling of nLDL and oxLDL with [^{18}F]SFB

Parameter	nLDL	[^{18}F]FB-nLDL	P nLDL vs [^{18}F]FB-nLDL	oxLDL	[^{18}F]FB-oxLDL	P oxLDL vs [^{18}F]FB-oxLDL	P nLDL vs oxLDL
REM	1	1.01 ± 0.04	ns	3.94 ± 0.23	3.91 ± 0.36	ns	0.000
Fluorescence intensity (360/430 nm, RF in %)	4.5 ± 0.4	4.6 ± 0.4	ns	24.3 ± 8.6	26.1 ± 9.1	ns	0.000
Total carbonyl groups (mol/mol apoB-100)	8.3 ± 0.3	8.2 ± 0.6	ns	14.6 ± 0.6	14.8 ± 0.6	ns	0.002
HAVA (mol/mol apoB-100)	0.009 ± 0.003	0.011 ± 0.003	ns	14.661 ± 0.884	14.044 ± 0.862	ns	0.000
HACA (mol/mol apoB-100)	0.0007 ± 0.0003	0.0007 ± 0.0003	ns	7.82 ± 1.62	7.86 ± 1.45	ns	0.000

Results are means ± SD (n = 10); Mann-Whitney U tests were used for comparison of numerical variables between groups

Importantly, for all parameters measured no significant differences were found between both radiolabelled nLDL and oxLDL particles and their non-radioactive counterparts. These results indicate, that under the pre-analytical and the coupling conditions employed, and in contrast to data on iodinated LDL as published by others, radiolabelling of LDL by [^{18}F]SFB did not lead either to adverse oxidation of nLDL particles or to additional adverse oxidative modification of oxLDL particles (Sobal et al., 2004).

The perpetuation of the biological activity of both radiolabelled [^{18}F]FB-nLDL and [^{18}F]FB-oxLDL *in vitro* was determined by cell binding and uptake studies as published elsewhere (Pietzsch et al., 2004c). In general, human hepatoma cell line HepG2 is considered the classic LDL receptor bearing cell type and is an accepted model for the examination of cellular binding and uptake of native LDL particles. On the other hand, when differentiated to macrophages after stimulation with phorbol esters, monocytic THP-1 cells are considered scavenger receptor bearing human cells and are an accepted model for the examination of cellular interaction with modified LDL, particularly oxLDL. In agreement with former results, the present binding experiments reveal a specific binding and uptake of [^{18}F]FB-nLDL to HepG2 cells and, on the other hand, a specific binding and uptake of [^{18}F]FB-oxLDL to THP-1 cells (Fig. 4). Molar excess (500 μg/mL) of unlabelled nLDL and oxLDL, respectively, essentially inhibited cellular binding and uptake of their corresponding radiolabelled analogues. On the other hand, native LDL does not appear to have any influence on the binding and uptake of oxLDL and *vice versa* (data not shown in detail). In the presence of either 10 μg/mL of polyinosinic acid (poly I) or 10 μg/mL fucoidan, two selective inhibitors of oxLDL binding to scavenger receptors of class A (SR-A), binding of oxLDL in THP-1 cells was inhibited by approximately 50%. As expected, residual binding and uptake of oxLDL after exposure to poly I and fucoidan, respectively, indicate that other scavenger receptors besides SR-A are involved or can compensate for interaction of THP-1 cells with oxLDL. The results further indicate that with respect to cellular binding and uptake radiolabelling of LDL by [^{18}F]SFB did not alter the biological activity and functionality of nLDL and oxLDL, respectively.

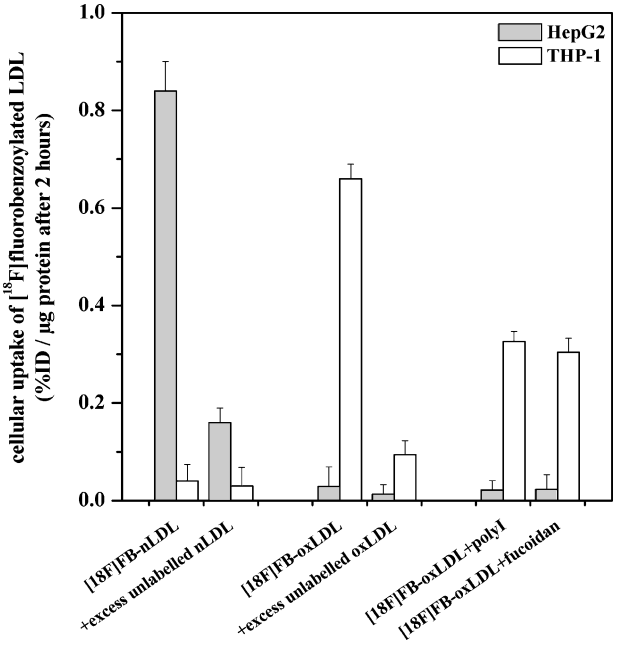

Fig. 4. Cellular uptake of [^{18}F]FB-nLDL and [^{18}F]FB-oxLDL after 2 hours in HepG2 cells (grey bars) and phorbol ester-stimulated THP-1 cells (white bars). For binding and cell association assays cells were incubated for 2 h at 4°C and 37°C, respectively, with either [^{18}F]FB-nLDL or [^{18}F]FB-oxLDL (2.5–50 μg of protein/mL in 125 μL of media with 50 mM Hepes, pH 7.4) in a total volume of 250 μL as published elsewhere (*cf.* (Pietzsch et al., 2004c). Non-specific binding was determined by the addition of an excess (500 μg/mL) of unlabelled nLDL and oxLDL, respectively, and represented less than 20% of total lipoprotein binding to both cell types. The extent of specific binding was calculated by subtracting the non-specific binding of [^{18}F]FB-nLDL and [^{18}F]FB-oxLDL, respectively, from total binding. Lipoprotein uptake for 2 hours was calculated as the difference between total cell-associated lipoprotein (37°C) and membrane-bound lipoprotein (4°C). Additionally, cellular uptake of [^{18}F]FB-oxLDL was studied in the presence of either 10 μg/mL of polyinosinic acid (poly I) or 10 μg/mL fucoidan. Results are expressed as means ± SD of five independent experiments

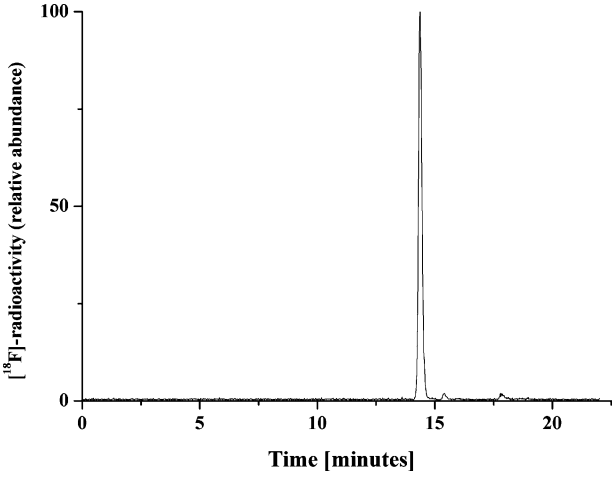

Fig. 5. Representative radiochromatogram of urine metabolite analysis 60 min after injection of [^{18}F]FB-oxLDL showing a dominant signal (retention time 14.4 min) ascribed to *N*-4-[^{18}F]fluorobenzoyl-glycine and minor unidentified metabolites at retention times 15.4 and 17.9 min, respectively

Table 2. Radioactivity, expressed as percent injected dose and percent injected dose per gram tissue, in different organs after single intravenous injection of 0.8–1.2 MBq [^{18}F]FB-nLDL and [^{18}F]FB-oxLDL, respectively

Organ	% ID				% ID/g of tissue			
	[^{18}F]FB-nLDL		[^{18}F]FB-oxLDL		[^{18}F]FB-nLDL		[^{18}F]FB-oxLDL	
	5 min *p.i.*	60 min *p.i.*	5 min *p.i.*	60 min *p.i.*	5 min *p.i.*	60 min *p.i.*	5 min *p.i.*	60 min *p.i.*
Blood	15.50 ± 4.60	10.82 ± 2.84	0.99 ± 0.15**	0.03 ± 0.01**	14.22 ± 2.00	10.40 ± 0.18	0.58 ± 0.09**	0.03 ± 0.01**
Brown fat	0.04 ± 0.02	0.05 ± 0.01	0.08 ± 0.04	0.01 ± 0.00	0.14 ± 0.01	0.11 ± 0.01	0.13 ± 0.04	0.03 ± 0.00
Brain	0.11 ± 0.02	0.06 ± 0.00	0.11 ± 0.02	0.01 ± 0.00	0.06 ± 0.02	0.04 ± 0.00	0.06 ± 0.01	0.01 ± 0.00
Pancreas	0.08 ± 0.03	0.08 ± 0.02	0.07 ± 0.06	0.01 ± 0.00	0.24 ± 0.12	0.17 ± 0.02	0.25 ± 0.04	0.03 ± 0.01
Spleen	0.55 ± 0.11	0.53 ± 0.08	0.09 ± 0.01**	0.01 ± 0.00**	3.09 ± 1.05	2.98 ± 1.15	0.17 ± 0.02**	0.06 ± 0.00**
Adrenals	0.17 ± 0.07	0.14 ± 0.01	0.02 ± 0.00**	0.01 ± 0.00**	3.70 ± 0.52	3.26 ± 0.18	0.36 ± 0.02**	0.09 ± 0.01**
Kidney	2.64 ± 1.13	3.11 ± 0.15	8.02 ± 0.06**	5.17 ± 0.08**	2.12 ± 0.19	2.74 ± 0.30	7.15 ± 0.49**	4.16 ± 0.69**
White fat	0.02 ± 0.00	0.02 ± 0.00	0.05 ± 0.03	0.01 ± 0.00	0.10 ± 0.05	0.07 ± 0.01	0.22 ± 0.11	0.03 ± 0.01
Muscle	0.04 ± 0.02	0.08 ± 0.01	0.09 ± 0.03	0.01 ± 0.00	0.06 ± 0.00	0.08 ± 0.03	0.05 ± 0.12	0.02 ± 0.01
Heart	0.17 ± 0.04	0.07 ± 0.01	0.16 ± 0.03	0.01 ± 0.00	0.34 ± 0.13	0.12 ± 0.01	0.26 ± 0.04	0.04 ± 0.02
Lung	0.92 ± 0.22	0.32 ± 0.09	0.43 ± 0.04*	0.03 ± 0.02**	0.79 ± 0.26	0.26 ± 0.01	0.39 ± 0.04*	0.01 ± 0.00**
Thymus	0.16 ± 0.02	0.09 ± 0.01	0.13 ± 0.02	0.01 ± 0.00	0.26 ± 0.01	0.16 ± 0.04	0.21 ± 0.03	0.02 ± 0.01
Thyroid gland	0.06 ± 0.02	0.02 ± 0.00	0.04 ± 0.02	0.01 ± 0.00	0.56 ± 0.22	0.24 ± 0.04	0.45 ± 0.05	0.13 ± 0.03
Harder glands	0.06 ± 0.03	0.04 ± 0.01	0.11 ± 0.07	0.02 ± 0.00	0.28 ± 0.10	0.17 ± 0.03	0.28 ± 0.09	0.09 ± 0.01
Liver	41.91 ± 2.99	35.96 ± 0.54	11.45 ± 0.97**	3.18 ± 0.55**	5.16 ± 1.71	4.63 ± 0.06	1.43 ± 0.08**	0.02 ± 0.00**
Femur	0.18 ± 0.04	0.15 ± 0.00	0.17 ± 0.01	0.18 ± 0.04	0.19 ± 0.06	0.19 ± 0.01	0.22 ± 0.02	0.18 ± 0.04
Testes	0.13 ± 0.09	0.07 ± 0.01	0.39 ± 0.19	0.07 ± 0.01	0.07 ± 0.03	0.03 ± 0.01	0.14 ± 0.08	0.02 ± 0.01
Intestine	1.47 ± 0.38	3.81 ± 1.00	5.70 ± 0.71**	8.56 ± 1.72	–	–	–	–
Urine	0.02 ± 0.00	47.93 ± 0.12	17.98 ± 0.26**	68.72 ± 2.40	–	–	–	–

Results are means ± SD (n = 8); Mann-Whitney U tests were used for comparison of numerical variables between groups

** $P < 0.01$ for differences between [^{18}F]FB-nLDL and [^{18}F]FB-oxLDL at corresponding time points

3.3 In vivo investigations

Radiochromatographic metabolite analysis of arterial blood samples confirmed high stability of both [^{18}F]FB-nLDL and [^{18}F]FB-oxLDL *in vivo*. At each time point after injection more than 96% of total blood [^{18}F]-radioactivity (decay-corrected) was recovered in the plasma protein pellet. In the plasma supernatants no low-molecular weight radioactive metabolites could be found. These data are in good agreement with those showing high *in vitro* stability of the [^{18}F]fluorobenzoylated LDL particles as a function of time in PBS and blood plasma at 37°C as published elsewhere (Pietzsch et al., 2004c). In contrast, urine analyses showed more than 98% of total urine [^{18}F]-radioactivity (decay-corrected) to be recovered in the urine supernatant indicating the formation of low-molecular weight radioactive metabolites. Subsequent HPLC analysis of urine supernatant showed up to three radioactive metabolites to be well separated under the conditions employed; retention times were very reproducible (Fig. 5). After injection of either [^{18}F]FB-nLDL or [^{18}F]FB-oxLDL the most abundant metabolite (maximum intensity reached approximately 90% of total [^{18}F]-radioactivity) is cleanly separated with a retention time of 14.4 min, the same retention time as of the reference compound *N*-4-[^{18}F]fluorobenzoyl-glycine. The minor metabolites (retention times were 15.4 and 17.9 min) have not been identified. However, free 4-[^{18}F]fluorobenzoic acid or [^{18}F]SFB was not detected.

Table 2 summarizes the distribution of [^{18}F]-radioactivity (decay-corrected) in male Wistar rats after a single intravenous injection of either [^{18}F]FB-nLDL or [^{18}F]FB-oxLDL. Data were obtained at 5 and 60 min post injection. Figures 6 and 7 show representative PET images of male Wistar rats after a single intravenous injection of either [^{18}F]FB-nLDL or [^{18}F]FB-oxLDL. Biodistribution studies revealed significant differences of both blood clearance and tissue association of [^{18}F]-radioactivity between [^{18}F]FB-nLDL and [^{18}F]FB-oxLDL (Table 2). These data could be confirmed by small animal PET studies. From these studies, time-activity-curves were obtained for the heart volume (majorily representing the cardiac blood pool), the liver, and the kidneys. The results from ROI analyses over these organs are given in Figs. 8A–C, and agree well with the corresponding results obtained from biodistribution experiments.

As a major result, after application of [^{18}F]FB-oxLDL, the disappearance of [^{18}F]-radioactivity concentration from the blood circulation proceeds at a very rapid rate. At 5 min after injection more than 90% of injected dose is already eliminated from the blood. Liver and kidneys are mainly responsible for this removal. At 5 min after injection approximately 12% of the injected dose is liver-associated. The [^{18}F]-radioactivity concentration within the liver declines very rapidly. A substantial fraction is cleared by the kidneys and approximately 8% of the injected dose is kidney-associated at 5 min *p.i.* The subsequent decline of [^{18}F]-radioactivity in the kidneys is delayed in comparison to the liver. Overall, fast systemic clearance of [^{18}F]-radioactivity after injection of [^{18}F]FB-oxLDL in the rat is explained by the rapid hepatobiliary and renal elimination of [^{18}F]-radioactivity.

In contrast to [^{18}F]FB-oxLDL, after first systemic passage, a significant amount of intact [^{18}F]FB-nLDL

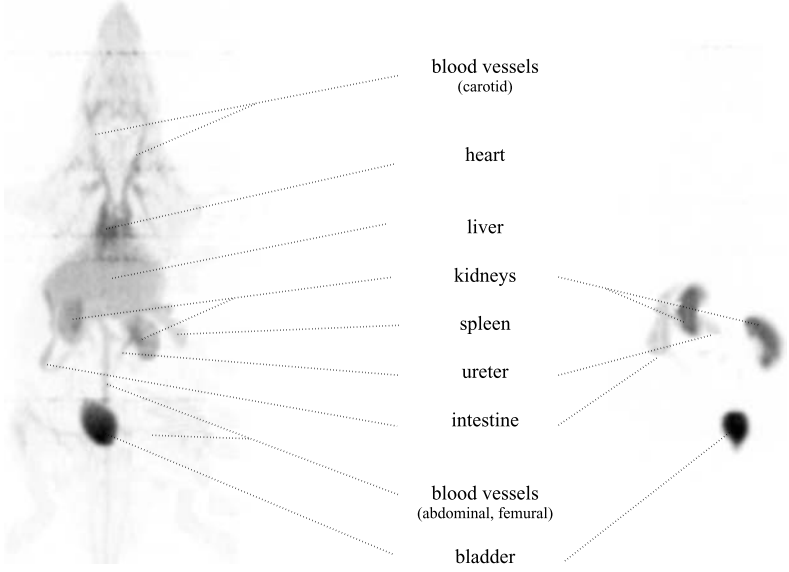

Fig. 6. Representative whole-body coronal images (maximum intensity projection) obtained from static small animal PET scans showing [^{18}F]-radioactivity distribution at 120 min after injection of [^{18}F]FB-nLDL (left) and [^{18}F]FB-oxLDL (right) in the sacrificed rat

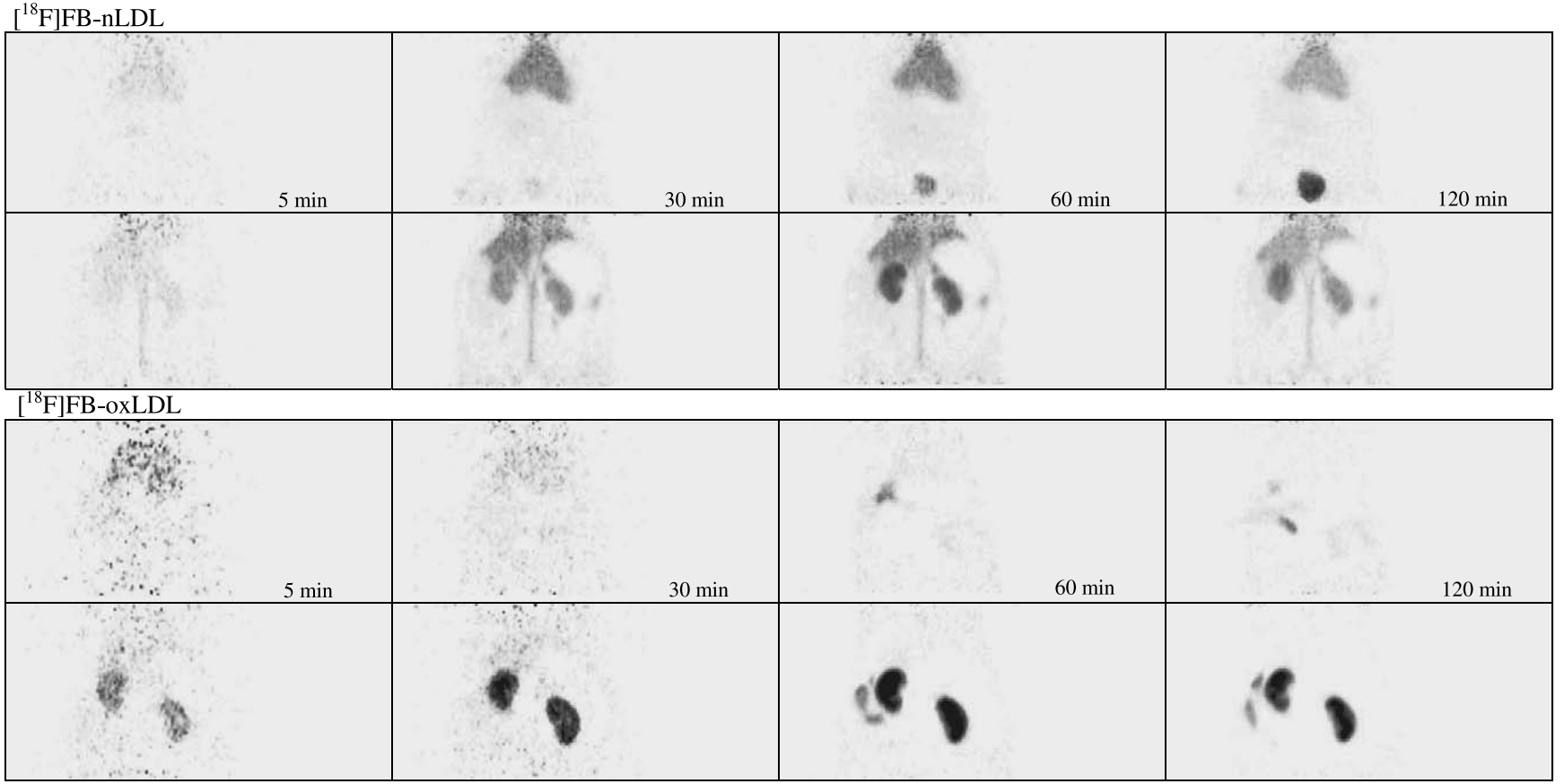

Fig. 7. Representative serial coronal images of abdominal region obtained from dynamic small animal PET scans showing [^{18}F]-radioactivity distribution at 5, 30, 60 and 120 min after injection of [^{18}F]FB-nLDL (top panel) and [^{18}F]FB-oxLDL (down panel) in the rat. Selected planes illustrate [^{18}F]-radioactivity entry into the liver (upper rows) and the kidneys (lower rows), respectively

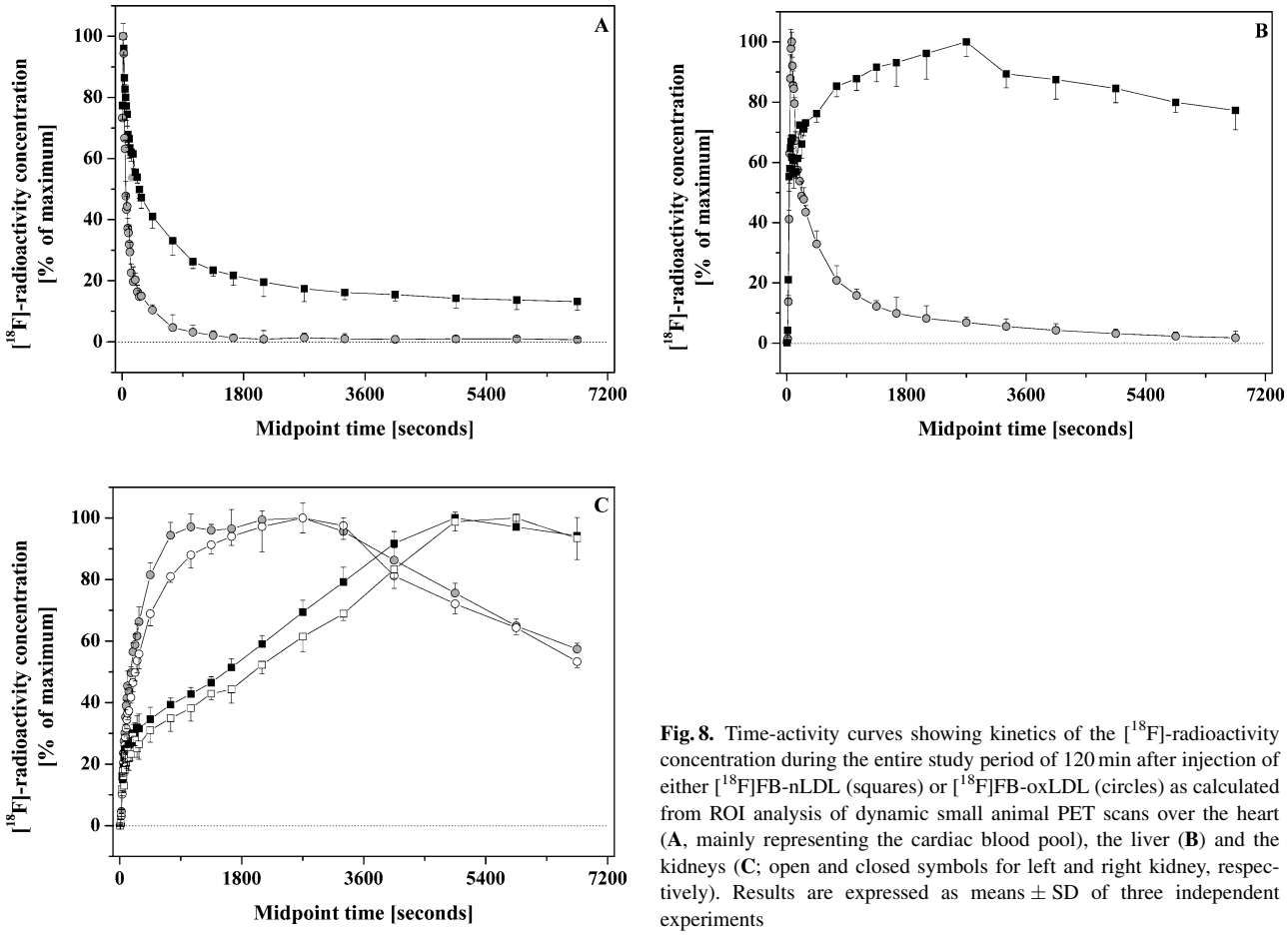

Fig. 8. Time-activity curves showing kinetics of the [^{18}F]-radioactivity concentration during the entire study period of 120 min after injection of either [^{18}F]FB-nLDL (squares) or [^{18}F]FB-oxLDL (circles) as calculated from ROI analysis of dynamic small animal PET scans over the heart (**A**, mainly representing the cardiac blood pool), the liver (**B**) and the kidneys (**C**; open and closed symbols for left and right kidney, respectively). Results are expressed as means ± SD of three independent experiments

remained in the circulation, amounting to 10% of the injected dose per mL at 60 min after injection. Assuming a total blood volume of approximately 4 to 5 mL this equals 40% to 50% of the injected dose. This is consistent with persisting pulmonary and splenic blood pools during the whole course of the study. The disappearance of [^{18}F]-radioactivity concentration from the blood circulation proceeds at a slower rate when compared with that of [^{18}F]FB-oxLDL. However, for this removal a progressive liver uptake is mainly responsible. At 5 min after injection approximately 42% of the injected dose is liver-associated. For the liver, an obvious temporary accumulation of [^{18}F]FB-nLDL was observable. Furthermore, a progressive uptake of [^{18}F]FB-nLDL in the kidneys also significantly contributes to blood clearance, but is strongly retarded when compared with the high kidney uptake and transit of [^{18}F]FB-oxLDL. On the other hand, uptake of [^{18}F]FB-nLDL in the kidneys occurred to considerably lower extent and rate than in the liver. In addition, a major fraction of [^{18}F]FB-nLDL showed uptake and temporary accumulation in the adrenal glands. On the other hand, the low mean accumulation of [^{18}F]-radioactivity in the femoral bone after 5 and 60 min, respectively, is indicative of a low *in vivo* defluorination of both [^{18}F]FB-LDL and [^{18}F]FB-oxLDL.

4 Discussion

The present work reports on continuing experiments on radiolabelling of apoB-100 of both native and oxidized LDL with the positron emitter [^{18}F] using the acylating reagent [^{18}F]SFB and the subsequent radiopharmacological characterization of [^{18}F]fluorobenzoylated LDL particles *in vitro* and *in vivo*. Radiolabelling with [^{18}F]SFB is considered to be a validated method for the incorporation of [^{18}F] into proteins and peptides as published by others and by ourselves (Vaidyanathan and Zalutsky, 1992; Wester et al., 1996; Bergmann et al., 2002; Wuest et al., 2003). For LDL apoB-100, our data indicate that radiolabelling with [^{18}F]SFB does not alter the biological activity and functionality of nLDL and oxLDL, respectively, *in vitro*. Of note, this radiolabelling procedure does not

lead either to adverse oxidation of nLDL particles or to additional adverse oxidative modification of oxLDL particles. Therefore, this methodology is supposed to provide a suitable radiotracer for differentiation of kinetics and metabolic fate of nLDL and oxLDL *in vivo*. This hypothesis could be confirmed by biodistribution experiments and dynamic small animal PET studies in rats.

In the past, radiohalogenation of proteins and lipoproteins has been established as an essential tool for assessment of their biological function *in vitro* and *in vivo* (Shepherd et al., 1976; Wilbur, 1992). Especially, the use of iodine radionuclides, principally iodine-125 and iodine-131, for labelling of proteins and lipoproteins is of widespread use. However, several authors showed that most commonly used oxidative radioiodination procedures such as iodogen, chloramine-T, or iodine monochloride lead to severe structural modifications of various proteins dramatically affecting their biological activity and functionality (Ganguly, 1987; Thibault et al., 1995; Bauer et al., 1996). Recently, for LDL the significant oxidative modification of both the lipid and the apolipoprotein moiety has been demonstrated (Khouw et al., 1993; Romero et al., 2001; Sobal et al., 2004). As strongly emphasized in these studies, it has to be considered that radioiodinated LDL no longer reflect the native LDL particle or, when obtained from *in vitro* oxidation experiments, the initially characterized modified LDL particle (Khouw et al., 1993; Romero et al., 2001; Sobal et al., 2004). Therefore, the valid use of iodinated LDL to reflect kinetics and behaviour of native LDL as well as to differentiate kinetics and behaviour of native and oxidized LDL are severely limited (Sobal et al., 2004). These limitations have to be considered for iodination of all proteins subjected to investigation of mechanisms and metabolic consequences of protein oxidation. Several attempts have been made to overcome adverse modification of proteins and lipoproteins by iodination such as the use of mild oxidizing reagents (Sinn et al., 1988), the use of antioxidants (Khouw et al., 1993), and the use of conjugative labelling employing Bolton-Hunter-type reagents (Wilbur, 1992; Ross et al., 1993; Frantzen et al., 1995). For the majority of proteins, the use of iodinated Bolton-Hunter-type reagents such as *N*-succinimidyl-3-(4-hydroxy-5-[^{125}I]iodophenyl)propionate or *N*-succinimidyl-4-[^{125}I]iodobenzoate is supposed to be a promising approach, because these *n.c.a.* systems for protein iodination prevent direct exposure of the protein to excess oxidizing and reducing agents. However, high incorporation of radioactivity into the LDL lipid moiety (>30%) limit the use of the majority of iodinated Bolton-Hunter-type reagents for radiolabelling of lipoproteins (Portman et al., 1976; Shepherd et al., 1976; Malmendier et al., 1988, Wilbur, 1992).

As an alternative, we propose the use of [^{18}F]SFB. Using this more hydrophilic fluorinated Bolton-Hunter-type reagent apoB-100, the major protein of LDL, can be specifically labelled via [^{18}F]fluorobenzoylation in the amino-terminus or the lysine side chain residues, respectively. As a result, the total radiochemical yields, effective specific radioactivities, and stability of [^{18}F]FB-nLDL and [^{18}F]FB-oxLDL, respectively, are sufficiently high for *in vitro* and *in vivo* investigations. Importantly, only trace amounts of ^{18}F radioactivity were incorporated into the lipid moiety of the radiolabelled LDL particles. More than 96% of the ^{18}F radioactivity was covalently coupled to apoB-100, the structural protein of LDL. The mature apoB-100 consists of a single polypeptide chain of 4536 amino acids, and there is only one copy of the protein on each LDL particle (Scott, 1989). Therefore, the metabolic fate of each LDL particle is paired for life with that of its apoB-100 molecule. ApoB-100 has 357 lysine side chain residues as well as its amino-terminus as possible sites for [^{18}F]fluorobenzoylation (Scott, 1989; Segrest et al., 2001). The amino-terminal region of apoB-100 is a hydrophilic, globular structure that extends away from the lipid core of the lipoprotein and is chemically accessible (Chan, 1992; Segrest et al., 2001; Yang et al., 2001). To minimize the number of different radiolabelled apoB-100 species, reaction conditions at pH 7.2 were used throughout, thus strictly favoring selective [^{18}F]-fluorobenzoylation at the amino-terminus of the apoB-100 molecule (Pietzsch et al., 2004c). As shown for free amino acids and a number of proteins, lysine side chain residues become the preferred site for conjugation with [^{18}F]SFB not until nearly complete deprotonation of the ε-amino group under basic conditions (Gaudriault et al., 1992; Bergmann et al., 2001; Johnstrom et al., 2002). For LDL, this has been confirmed by reacting LDL particles with stoichiometric amounts of unlabelled [^{19}F]SFB and measurement of coupled 4-fluorobenzoic acid residues to different domains of apoB-100 using specific and sensitive gas chromatography-mass spectrometry methodology (Oltmanns et al., 1989; Pietzsch and Julius, 2001). Data suggest that lysine side chain residues were nearly completely unreactive under the conditions employed, and, on the other hand, the position of the radiolabel is the amino-terminus in apoB-100 (Pietzsch et al., 2004c).

The ability to study the kinetics of lipoprotein metabolism in both animal models of disease and human *in vivo* using iodinated autologous and homologous LDL has

added significantly to our understanding of the regulation of plasma lipid levels in normal and dyslipidemic subjects (Burnett and Barrett, 2002). However, with respect to the investigation of the metabolism of oxidized LDL *in vivo*, the use of radioiodine has some inherent limitations, e.g., over- or underestimation of fractional catabolic rates. The relevance of these limitations varies greatly depending on the type of studies being performed and the types of modified lipoproteins being studied (Ramakrishnan et al., 1990; van Berkel et al., 1991; Atsma et al., 1991; Khouw et al., 1993; Ling et al., 1997; Romero et al., 2001; Sobal et al., 2004). Other approaches, e.g., using endogenous labelling of LDL apoB-100 with stable isotope amino acids, are limited in direct metabolic differentiation of native and modified LDL and are virtually inapplicable in small animal models (Pietzsch et al., 2000).

Fortunately, these limitations can be essentially eliminated by the use of the present methodology. Our data demonstrate that the use of [^{18}F]SFB for radiolabelling of LDL does not affect native and modified LDL specimen by initial or further oxidative modification or, with respect to specific receptor-mediated cellular binding and uptake, by alteration of their biological function *in vitro*. Consequently, we hypothesized these findings to be sufficient to allow the use of [^{18}F]FB-nLDL and [^{18}F]FB-oxLDL in biodistribution experiments and dynamic small animal PET studies *in vivo*.

As expected, in rats the major binding site of [^{18}F]FB-nLDL particles is in the liver. Rat hepatocytes express a high number of LDL receptors that specifically bind to human nLDL, even if human LDL show a lower affinity to rat hepatocytes than rat LDL (Corsini et al., 1992). Furthermore, interaction between apoB-100 and hepatic lipase (HL) facilitates the LDL receptor-mediated uptake of nLDL by cells where HL is present, such as hepatocytes and endothelial cells lining hepatic sinusoids and the adrenal glands, respectively (Choi et al., 1998). This is also consistent with our results which show a comparably high uptake of nLDL in adrenal glands. Moreover, an abundant binding of nLDL in the kidneys could be observed. This may be explained by the specific uptake of human nLDL in rat glomerular and, preferentially, mesangial epithelial cells by LDL receptors (Zheng et al., 1994; Groene et al., 1990; Grone et al., 1992). On the other hand, during the whole study period of either 60 min for biodistribution experiments or 120 min for dynamic small animal PET studies a significant fraction of circulating intact [^{18}F]FB-nLDL particles remained in the blood compartment. This is also reflected by the persisting pulmonary and spleenic blood pool of [^{18}F]FB-nLDL. As a first approximation, the observed residence time of circulating human nLDL in rat blood compartment is consistent with data from the literature.

In contrast, [^{18}F]FB-oxLDL particles are nearly completely cleared from the blood compartment within the first 5 min after injection. During this time a major fraction of oxLDL is very rapidly cleared in the rat liver. This behavior could be expected from findings reported by others and, to the major part, is ascribed to scavenger receptors class A (SR AI/AII) that are highly expressed in Kupffer cells and sinusoidal endothelial cells, respectively (van Berkel et al., 1991, Dhaliwal and Steinbrecher, 1999; Terpstra et al., 2000). Of note, both Kupffer and sinusoidal endothelial cells represent the hepatic reticuloendothelial system (RES), as initially launched by Aschoff (Aschoff, 1924). In rats the hepatic RES is considered to be the most important site of elimination of nearly all tested soluble waste macromolecules including modified LDL (Blomhoff et al., 1984; Seternes et al., 2002; Nedredal et al., 2003). In addition to SR-A, rat Kupffer cells highly express macrosialin (the rodent homologue of human CD68) and the class B scavenger receptor CD-36 that are also able to recognize oxLDL (de Rijke et al., 1994; van Velzen et al., 1997; Terpstra et al., 2000). These assumptions are consistent with the *in vitro* finding showing cellular uptake of [^{18}F]FB-oxLDL in THP-1 cells to be inhibited only by approximately 50% in the presence of either poly I or fucoidan. Poly I and fucoidan are structurally different negatively charged compounds that specifically compete with oxidatively modified apoB-100 for binding to SR-A (Wang et al., 2001). Their inhibition effect is attributed to their negative charge indicating that binding of [^{18}F]FB-oxLDL to THP-1 cells in part is mediated by oxidation-specific negatively charged epitopes in oxLDL. As published by others, after inhibition or deficiency of SR-A in THP-1 cells majorily macrosialin and, to a minor extent, CD-36 can compensate for recognition of oxLDL (Endemann et al., 1993; Ramprasad et al., 1996; Wang et al., 2001; Sugano et al., 2001).

Of interest, in the present study a substantial fraction of oxLDL is also cleared in the kidneys. It has been shown that most vertebrates have so-called scavenger endothelial cells (endothelial cells endowed with the same RES-function as sinusoidal endothelial cells) also in organs other than the liver (Seternes et al., 2002). In particular, these scavenger endothelial cells are also geared to endocytosis of oxLDL. Their arsenal comprises several classes of scavenger receptors distinct from the class A that, in an alternating fashion, also stand in for specific oxLDL

recognition and uptake. In rat kidneys, these endothelial cell-scavenger receptors mainly comprise the lectin-like receptor, LOX-1 (Ueno et al., 2003). Furthermore, rat glomerular mesangial cells that also express scavenger receptors like LOX-1 further contribute to oxLDL recognition and uptake in the kidneys (Schlondorff, 1993; Lee and Koh, 1994; Draude et al., 1999).

Our observations are further supported by metabolite analysis. In the present study, after intravenous application of [^{18}F]FB-nLDL or [^{18}F]FB-oxLDL no radioactive metabolites were determined in plasma samples. At each time point of analysis, more than 96% of total blood [^{18}F]-radioactivity (decay-corrected) can be ascribed to either intact [^{18}F]FB-nLDL or [^{18}F]FB-oxLDL. On the other hand, in urine samples low-molecular weight metabolites were found. At 60 min after injection, more than 90% of total [^{18}F]-radioactivity (decay-corrected) in urine can be ascribed to the formation of *N*-4-[^{18}F]fluorobenzoyl-glycine (4-[^{18}F]fluorohippuric acid). It is suggested that, like other 4-halobenzoic acids, *N*-4-[^{18}F]fluorobenzoyl-glycine is formed by biotransformation of free 4-[^{18}F]fluorobenzoic acid by ATP-dependent acyl-CoA synthetase and acylCoA:glycine *N*-acyltransferase, a process that occurs mainly in rat liver and kidneys, followed by excretion without further biotransformation in the bile and urine, respectively (Poon and Pang, 1995; Laznicek and Laznickova, 1999; Corcoran et al., 1999; Schwab et al., 2001). It is likely that free 4-[^{18}F]fluorobenzoic acid becomes available for this process after endocytosis and lysosomal degradation of apoB-100 of [^{18}F]FB-nLDL and [^{18}F]FB-oxLDL, respectively. Additionally, in urine one to two other radioactive metabolites could be found showing low abundance (each $<$10% of total [^{18}F]-radioactivity) and indicating further minor metabolic pathways for 4-[^{18}F]fluorobenzoic acid or [^{18}F]FB-labelled amino acids. These pathways await further investigation but possibly include the formation as well as hepatic and renal handling of 4-[^{18}F]fluorobenzoyl glucuronides or sulphates (Ghauri et al., 1992; Corcoran et al., 1999; Ishii et al., 2002).

In summary, keeping in mind the intrinsic properties of PET and the continuous developments of this technique, particularly small animal PET, radiolabelling of LDL with [^{18}F]SFB represents a promising approach for characterization and discrimination of the kinetics and the metabolic fate of native LDL and oxidatively modified LDL *in vivo*. Our data show that in the rat both liver and kidney form an efficient scavenger apparatus to remove oxLDL modified by hemin-induced oxidation from the circulation, thus protecting the organism against the atherogenic action of these oxLDL in the blood compartment. From the literature and the present *in vitro* and *in vivo* data we suppose resident macrophages and endothelial cells in both liver and kidney to be responsible for rapid and complete scavenging of oxLDL. Of note, the 109.8 min half-life of ^{18}F may limit its use for some applications. However, the present methodology allows syntheses, plasma and metabolite analysis, and imaging procedures that can be extended up to 6 h. This particularly facilitates kinetic studies in a metabolic setting with a comparatively fast LDL turnover, as is the case in most animal models, including rodent models of disease (e.g., mice and rats prone to atherosclerosis) (Bocan, 1998; Herrera et al., 1999).

Considering the heterogeneity of oxidant processes of sizable physiological relevance, e.g., transition metal catalyzed oxidation, myeloperoxidase catalyzed reactions, nitrosative or glycative stress, additional work is needed to understand the nature of the original oxidative insult. In this study, as a well-characterized experimental model for transition metal catalyzed oxidation, *in vitro* oxidation of LDL apoB-100 in the presence of the pro-oxidant hemin (Fe^{3+}-protoporphyrin IX) was selected (Camejo et al., 1998; Pietzsch, 2000; Pietzsch and Bergmann, 2004). Hemin is a blood product and a source of iron. Free transition metals like iron and copper are strong catalysts for oxidation reactions in the presence of hydroperoxides (Welch et al., 2002; Gaetke and Chow, 2003). Because the availability of free copper or iron *in vivo* is very low and under tight control, the hemin model is considered to be of high pathophysiological relevance (Grinberg et al., 1999; Rae et al., 1999; Miller and Shaklai, 1999; Jeney et al., 2002; Pietzsch and Bergmann, 2004). In this line, major specific products of transition metal catalyzed oxidation of positively charged protein amino acids are γ-glutamyl-semialdehyde (γGSA) and α-aminoadipyl-semialdehyde (αASA). Oxidation of LDL apoB-100 proline and arginine residues to γGSA, which by reduction forms 5-hydroxy-2-aminovaleric acid (HAVA), and oxidation of LDL apoB-100 lysine residues to αASA, which by reduction forms 6-hydroxy-2-aminocaproic acid (HACA), has been demonstrated *in vitro* (Pietzsch, 2000; Pietzsch and Bergmann, 2004). Very recently, the concentrations of HAVA and HACA in LDL apoB-100 were demonstrated to be higher in LDL from early, intermediate, and advanced atherosclerotic lesions, when compared with LDL from normal aortic tissue (Pietzsch et al., 2004a). Moreover, levels of HAVA and HACA were significantly higher in circulating LDL recovered from subjects who were at high atherosclerotic risk (Pietzsch et al., 2000,

2004b; Julius and Pietzsch, in press). These findings strongly support the hypothesis that pathways involving transition metal catalyzed oxidation of LDL apoB-100 are of pathophysiological significance for atherogenesis.

Furthermore, the magnitude of oxidative modification is of ample importance. It has to be noticed that the oxLDL particles used in the present study represent massively modified LDL particles. Assuming that in the living organism oxLDL particles with a comparable extent of oxidation may enter the circulation, e.g., by backward diffusion from stable subendothelial atherosclerotic lesions, by release from unstable plaques, or by diffusion from inflammatory sites such as inflamed joints, these massively modified LDL particles should be rapidly removed from the blood by the mechanisms discussed above. This would explain the very low levels of such massively modified LDL particles in the circulation when compared to other compartments like the arterial wall. On the other hand, it is more likely that circulating oxLDL comprise also particles with a lesser extent of oxidation including the so-called minimally modified LDL that are in part still recognized via the LDL receptor. To evaluate a possible clinical significance of these different entities of modified LDL further investigations are necessary. These investigations should also provide information about the impact of pathways of detoxification of food ingredients or the influence of lipid-soluble dietary antioxidants, e.g., tocopherols and polyphenols, on LDL oxidation and *in vivo* metabolism of LDL (Frei and Higdon, 2003).

Acknowledgements

The authors are grateful to Ms. Mareike Barth and Ms. Katrin Rode for their expert technical assistance in human LDL preparation and characterization. We are also grateful to Mrs. Sigrid Nitzsche from the Lipoprotein Laboratory at the Department of Internal Medicine 3, Carl Gustav Carus Medical School, University of Technology Dresden, for her expert advice and many stimulating discussions.

References

Aschoff L (1924) Das Reticulo-Endotheliale System. Ergeb Inn Med Kinderhk 26: 1–118

Atsma DE, Kempen HJ, Nieuwenhuizen W, van't Hooft FM, Pauwels EK (1991) Partial characterization of low density lipoprotein preparations isolated from fresh and frozen plasma after radiolabeling by seven different methods. J Lipid Res 32: 173–181

Barrett HP, Foster DM (1996) Design and analysis of lipid tracer kinetic studies. Curr Opin Lipidol 7: 143–148

Bauer RJ, Leigh SD, Birr CA, Bernhard SL, Fang M, Der K, Ihejeto NO, Carroll SF, Kung AH (1996) Alteration of the pharmacokinetics of small proteins by iodination. Biopharm Drug Dispos 17: 761–774

Bergmann R, Helling R, Heichert C, Scheunemann M, Mading P, Wittrisch H, Johannsen B, Henle T (2001) Radio fluorination and positron emission tomography (PET) as a new approach to study the *in vivo* distribution and elimination of the advanced glycation end-products N-epsilon-carboxymethyllysine (CML) and N-epsilon-carboxyethyllysine (CEL). Nahrung 45: 182–188

Bergmann R, Scheunemann M, Heichert C, Mading P, Wittrisch H, Kretzschmar M, Rodig H, Tourwe D, Iterbeke K, Chavatte K, Zips D, Reubi JC, Johannsen B (2002) Biodistribution and catabolism of (18)F-labeled neurotensin(8–13) analogs. Nucl Med Biol 29: 61–72

Bjornheden T, Bondjers G, Wiklund O (1998) Direct assessment of lipoprotein outflow from *in vivo*-labeled arterial tissue as determined in an *in vitro* perfusion system. Arterioscler Thromb Vasc Biol 18: 1927–1933

Blomhoff R, Drevon CA, Eskild W, Helgerud P, Norum KR, Berg T (1984) Clearance of acetyl low density lipoprotein by rat liver endothelial cells. Implications for hepatic cholesterol metabolism. J Biol Chem 259: 8898–8903

Bocan TM (1998) Animal models of atherosclerosis and interpretation of drug intervention studies. Curr Pharm Des 4: 37–52

Burnett JR, Barrett PH (2002) Apolipoprotein B metabolism: tracer kinetics, models, and metabolic studies. Crit Rev Clin Lab Sci 39: 89–137

Camejo G, Halberg C, Manschik-Lundin A, Hurt-Camejo E, Rosengren B, Olsson H, Hansson GI, Forsberg GB, Ylhen B (1998) Hemin binding and oxidation of lipoproteins in serum: mechanisms and effect on the interaction of LDL with human macrophages. J Lipid Res 39: 755–766

Chan L (1992) Apolipoprotein B, the major protein component of triglyceride-rich and low density lipoproteins. J Biol Chem 267: 25621–25624

Chang MY, Lees AM, Lees RS (1993) Low-density lipoprotein modification and arterial wall accumulation in a rabbit model of atherosclerosis. Biochemistry 32: 8518–8524

Choi SY, Goldberg IJ, Curtiss LK, Cooper AD (1989) Interaction between ApoB and hepatic lipase mediates the uptake of ApoB-containing lipoproteins. J Biol Chem 273: 20456–20462

Corcoran O, Wilson ID, Nicholson JK (1999) Rapid multi-component detection of fluorinated drug metabolites in whole urine from a 'cassette' dose study using high resolution ^{19}F NMR spectroscopy. Anal Commun 36: 259–261

Corsini A, Mazzotti M, Villa A, Maggi FM, Bernini F, Romano L, Romano C, Fumagalli R, Catapano AL (1992) Ability of the LDL receptor from several animal species to recognize the human apo B binding domain: studies with LDL from familial defective apo B-100. Atherosclerosis 93: 95–103

Defrise M, Kinahan PE, Townsend DW, Michel C, Sibomana M, Newport DF (1997) Exact and approximate rebinning algorithms for 3-D PET data. IEEE Trans Med Imaging 16: 145–158

De Rijke YB, Biessen EA, Vogelezang CJ, van Berkel TJ (1994) Binding characteristics of scavenger receptors on liver endothelial and Kupffer cells for modified low-density lipoproteins. Biochem J 304: 69–73

Dhaliwal BS, Steinbrecher UP (1999) Scavenger receptors and oxidized low density lipoproteins. Clin Chim Acta 286: 191–205

Draude G, Hrboticky N, Lorenz RL (1999) The expression of the lectin-like oxidized low-density lipoprotein receptor (LOX-1) on human vascular smooth muscle cells and monocytes and its down-regulation by lovastatin. Biochem Pharmacol 57: 383–386

Endemann G, Stanton LW, Madden KS, Bryant CM, White RT, Protter AA (1993) CD36 is a receptor for oxidized low density lipoprotein. J Biol Chem 268: 11811–11816

Frantzen F, Heggli DE, Sundrehagen E (1995) Radiolabelling of human haemoglobin using the 125I-Bolton-Hunter reagent is superior to oxidative iodination for conservation of the native structure of the labelled protein. Biotechnol Appl Biochem 22: 161–167

Frei B, Higdon JV (2003) Antioxidant activity of tea polyphenols *in vivo*: evidence from animal studies. J Nutr 133: 3275S–3284S

Gaetke LM, Chow CK (2003) Copper toxicity, oxidative stress, and antioxidant nutrients. Toxicology 189: 147–163

Ganguly S (1987) Iodination-induced alterations in biochemical properties of human placental insulin receptor. FEBS Lett 224: 198–200

Ghauri FY, Blackledge CA, Glen RC, Sweatman BC, Lindon JC, Beddell CR, Wilson ID, Nicholson JK (1992) Quantitative structure-metabolism relationships for substituted benzoic acids in the rat. Computational chemistry, NMR spectroscopy and pattern recognition studies. Biochem Pharmacol 44(10): 1935–1946

Gaudriault G, Vincent JP (1992) Selective labeling of alpha- or epsilon-amino groups in peptides by the Bolton-Hunter reagent. Peptides 13: 1187–1192

Grinberg LN, O'Brien PJ, Hrkal Z (1999) The effects of heme-binding proteins on the peroxidative and catalatic activities of hemin. Free Radic Biol Med 27: 214–219

Grone HJ, Walli AK, Grone E, Kramer A, Clemens MR, Seidel D (1990) Receptor mediated uptake of apo B and apo E rich lipoproteins by human glomerular epithelial cells. Kidney Int 37: 1449–1459

Grone EF, Abboud HE, Hohne M, Walli AK, Grone HJ, Stuker D, Robenek H, Wieland E, Seidel D (1992) Actions of lipoproteins in cultured human mesangial cells: modulation by mitogenic vasoconstrictors. Am J Physiol 263: F686–F696

Heinecke JW (2002) Oxidized amino acids: culprits in human atherosclerosis and indicators of oxidative stress. Free Radic Biol Med 32: 1090–1101

Herrera VL, Makrides SC, Xie HX, Adari H, Krauss RM, Ryan US, Ruiz-Opazo N (1999) Spontaneous combined hyperlipidemia, coronary heart disease and decreased survival in Dahl salt-sensitive hypertensive rats transgenic for human cholesteryl ester transfer protein. Nat Med 5: 1383–1389

Ishii M, Kanayama M, Esumi H, Ogawara KI, Kimura T, Higaki K (2002) Pharmacokinetic analysis of factors determining elimination pathways for sulfate and glucuronide metabolites of drugs. I: studies by *in vivo* constant infusion. Xenobiotica 32: 441–450

Jeney V, Balla J, Yachie A, Varga Z, Vercellotti GM, Eaton JW, Balla G (2002) Pro-oxidant and cytotoxic effects of circulating heme. Blood 100: 879–887

Johnstrom P, Harris NG, Fryer TD, Barret O, Clark JC, Pickard JD, Davenport AP (2002) (18)F-Endothelin-1, a positron emission tomography (PET) radioligand for the endothelin receptor system: radiosynthesis and *in vivo* imaging using microPET. Clin Sci 103 [Suppl 48]: 4S–8S

Julius U, Pietzsch J (2005) Specific enhancement by glucose of hemin catalyzed LDL oxidation *in vitro* and *in vivo*. Antiox Redox Signal (in press)

Khouw AS, Parthasarathy S, Witztum JL (1993) Radioiodination of low density lipoprotein initiates lipid peroxidation: protection by use of antioxidants. J Lipid Res 34: 1483–1496

Kopprasch S, Leonhardt W, Pietzsch J, Kuhne H (1998) Hypochlorite-modified low-density lipoprotein stimulates human polymorphonuclear leukocytes for enhanced production of reactive oxygen metabolites, enzyme secretion, and adhesion to endothelial cells. Atherosclerosis 136: 315–324

Laznicek M, Laznickova A (1999) Renal handling of iodobenzoates in rats. J Pharm Pharmacol 51: 1019–1023

Lee HS, Koh HI (1994) Visualization of binding and uptake of oxidized low density lipoproteins by cultured mesangial cells. Lab Invest 71: 200–208

Ling W, Lougheed M, Suzuki H, Buchan A, Kodama T, Steinbrecher UP (1997) Oxidized or acetylated low density lipoproteins are rapidly cleared by the liver in mice with disruption of the scavenger receptor class A type I/II gene. J Clin Invest 100: 244–252

Liu X, Comtat C, Michel C, Kinahan P, Defrise M, Townsend D (2001) Comparison of 3-D reconstruction with 3D-OSEM and with FORE + OSEM for PET. IEEE Trans Med Imaging 20: 804–814

Malmendier CL, Lontie JF, Grutman GA, Delcroix C (1988) Metabolism of apolipoprotein C-III in normolipemic human subjects. Atherosclerosis 69: 51–59

Miller YI, Shaklai N (1999) Kinetics of hemin distribution in plasma reveals its role in lipoprotein oxidation. Biochim Biophys Acta 1454: 153–164

Nedredal GI, Elvevold KH, Ytrebo LM, Olsen R, Revhaug A, Smedsrod B (2003) Liver sinusoidal endothelial cells represents an important blood clearance system in pigs. Comp Hepatol 2: 1–14

Oltmanns RH, Muller R, Otto MK, Lingens F (1989) Evidence for a new pathway in the bacterial degradation of 4-fluorobenzoate. Appl Environ Microbiol 55: 2499–2504

Ottnad E, Via DP, Frubis J, Sinn H, Friedrich E, Ziegler R, Dresel HA (1992) Differentiation of binding sites on reconstituted hepatic scavenger receptors using oxidized low-density lipoprotein. Biochem J 281: 745–751

Pietzsch J (2000) Measurement of 5-hydroxy-2-aminovaleric acid as a specific marker of iron-mediated oxidation of proline and arginine side-chain residues of low-density lipoprotein apolipoprotein B-100. Biochem Biophys Res Commun 270: 852–857

Pietzsch J, Bergmann R (2003) Measurement of 5-hydroxy-2-aminovaleric acid as a specific marker of metal catalysed oxidation of proline and arginine residues of low density lipoprotein apolipoprotein B-100 in human atherosclerotic lesions. J Clin Pathol 56: 622–623

Pietzsch J, Bergmann R (2004) Analysis of 6-hydroxy-2-aminocaproic acid (HACA) as a specific marker of protein oxidation: the use of N(O,S)-ethoxycarbonyl trifluoroethyl ester derivatives and gas chromatography/mass spectrometry. Amino Acids 26: 45–51

Pietzsch J, Julius U (2001) Different susceptibility to oxidation of proline and arginine residues of apolipoprotein B-100 among subspecies of low density lipoproteins. FEBS Lett 491: 123–126

Pietzsch J, Subat S, Nitzsche S, Leonhardt W, Schentke KU, Hanefeld M (1995) Very fast ultracentrifugation of serum lipoproteins: influence on lipoprotein separation and composition. Biochim Biophys Acta 1254: 77–88

Pietzsch J, Lattke P, Julius U (2000) Oxidation of apolipoprotein B-100 in circulating LDL is related to LDL residence time. *In vivo* insights from stable-isotope studies. Arterioscler Thromb Vasc Biol 20: E63–E67

Pietzsch J, Bergmann R, Kopprasch S (2004a) Analysis of non-protein amino acids as specific markers of low density lipoprotein apolipoprotein B-100 oxidation in human atherosclerotic lesions: the use of N(O)-ethoxycarbonyl trifluoroethyl ester derivatives and GC-MS. Spectroscopy 18: 177–183

Pietzsch J, Bergmann R, Kopprasch S (2004b) Analysis of specific markers of protein oxidation in rheumatoid arthritis plasma and synovial fluid LDL. Atherosclerosis 5 [Suppl 1]: 16

Pietzsch J, Bergmann R, Rode K, Hultsch C, Pawelke B, Wuest F, van den Hoff J (2004c) Fluorine-18 radiolabeling of low density lipoproteins (LDL): a potential approach for characterization and differentiation of metabolism of native and oxidized LDL *in vivo*. Nucl Med Biol 31: 1043–1050

Poetzsch C, Beuthien-Baumann B, van den Hoff J (2003) Teilautomatisierte Segmentierung zur Quantifizierung von Metastasen bei der FDG-PET. Nuklearmedizin 42: 26

Poon K, Pang KS (1995) Benzoic acid glycine conjugation in the isolated perfused rat kidney. Drug Metab Dispos 23: 255–260

Portman OW, Alexander M, Tanaka N, Soltys P (1976) The effects of dietary fat and cholesterol on the metabolism of plasma low density lipoprotein apoproteins in squirrel monkeys. Biochim Biophys Acta 450: 185–196

Rae TD, Schmidt PJ, Pufahl RA, Culotta VC, O'Halloran TV (1999) Undetectable intracellular free copper: the requirement of a copper chaperone for superoxide dismutase. Science 284: 805–808

Ramakrishnan R, Arad Y, Wong S, Ginsberg HN (1990) Nonuniform radiolabeling of VLDL apolipoprotein B: implications for the analysis of studies of the kinetics of the metabolism of lipoproteins containing apolipoprotein B. J Lipid Res 31: 1031–1042

Ramprasad MP, Terpstra V, Kondratenko N, Quehenberger O, Steinberg D (1996) Cell surface expression of mouse macrosialin and human CD68 and their role as macrophage receptors for oxidized low density lipoprotein. Proc Natl Acad Sci USA 93: 14833–14838

Raymond TL, Reynolds SA, Swanson JA (1986) Turnover of low-density lipoprotein isolated from interstitial inflammatory fluid of the rabbit. Inflammation 10: 93–98

Romero JR, Martinez R, Fresnedo O, Ochoa B (2001) Comparison of two methods for radioiodination on the oxidizability properties of low density lipoprotein. J Physiol Biochem 57: 291–301

Ross R (1999) Atherosclerosis – an inflammatory disease. N Engl J Med 340: 115–126

Ross J, Janero DR, Hreniuk D, Wennogle LP (1993) Radioiodination of transforming growth factor-beta (TGF-beta) in a modified Bolton-Hunter reaction system. J Biochem Biophys Methods 26: 343–350

Sasaki J, Cottam GL (1982) Glycosylation of LDL decreases its ability to interact with high-affinity receptors of human fibroblasts *in vitro* and decreases its clearance from rabbit plasma *in vivo*. Biochim Biophys Acta 713: 199–207

Schlondorff D (1993) Cellular mechanisms of lipid injury in the glomerulus. Am J Kidney Dis 22: 72–82

Schwab AJ, Tao L, Yoshimura T, Simard A, Barker F, Pang KS (2001) Hepatic uptake and metabolism of benzoate: a multiple indicator dilution, perfused rat liver study. Am J Physiol Gastrointest Liver Physiol 280: G1124–G1136

Scott J (1989) The molecular and cell biology of apolipoprotein-B. Mol Biol Med 6: 65–80

Segrest JP, Jones MK, De Loof H, Dashti N (2001) Structure of apolipoprotein B-100 in low density lipoproteins. J Lipid Res 42: 1346–1367

Seternes T, Sorensen K, Smedsrod B (2002) Scavenger endothelial cells of vertebrates: a nonperipheral leukocyte system for high-capacity elimination of waste macromolecules. Proc Natl Acad Sci USA 99: 7594–7597

Shaish A, Keren G, Chouraqui P, Levkovitz H, Harats D (2001) Imaging of aortic atherosclerotic lesions by (125)I-LDL, (125)I-oxidized-LDL, (125)I-HDL and (125)I-BSA. Pathobiology 69: 225–229

Shepherd J, Bedford DK, Morgan HG (1976) Radioiodination of human low density lipoprotein: a comparison of four methods. Clin Chim Acta 66: 97–109

Sies H (1985) Introductory remarks. In: Sies H (ed) Oxidative stress. Academic Press, Orlando, FL, pp 1–7

Sinn HJ, Schrenk HH, Friedrich EA, Via DP, Dresel HA (1988) Radioiodination of proteins and lipoproteins using N-bromosuccinimide as oxidizing agent. Anal Biochem 170: 186–192

Sobal G, Resch U, Sinzinger H (2004) Modification of low-density lipoprotein by different radioiodination methods. Nucl Med Biol 31: 381–388

Stadtman ER, Berlett BS (1998) Reactive oxygen-mediated protein oxidation in aging and disease. Drug Metab Rev 30: 225–243

Stadtman ER, Levine RL (2003) Free radical-mediated oxidation of free amino acids and amino acid residues in proteins. Amino Acids 25: 207–218

Stocker R, Keaney JF (2004) Role of oxidative modifications in atherosclerosis. Physiol Rev 84: 1381–1478

Sugano R, Yamamura T, Harada-Shiba M, Miyake Y, Yamamoto A (2001) Uptake of oxidized low-density lipoprotein in a THP-1 cell line lacking scavenger receptor A. Atherosclerosis 158: 351–357

Terpstra V, van Amersfoort ES, van Velzen AG, Kuiper J, van Berkel TJC (2000). Hepatic and extrahepatic scavenger receptors: function in relation to disease. Arterioscler Thromb Vasc Biol 20: 1860–1872

Thibault G, Grove KL, Deschepper CF (1995) Reduced affinity of iodinated forms of Tyr0 C-type natriuretic peptide for rat natriuretic peptide receptor B. Mol Pharmacol 48: 1046–1053

Ueno T, Kaname S, Takaichi K, Nagase M, Tojo A, Onozato ML, Fujita T (2003) LOX-1, an oxidized low-density lipoprotein receptor, was upregulated in the kidneys of chronic renal failure rats. Hypertens Res 26: 117–122

Vaidyanathan G, Zalutsky MR (1992) Labeling proteins with fluorine-18 using N-succinimidyl 4-[18F]fluorobenzoate. Int J Radiat Appl Instrum B 19: 275–281

Van Berkel TJC, De Rijke YB, Kruijt JK (1991) Different fate *in vivo* of oxidatively modified low density lipoprotein and acetylated low density lipoprotein in rats. Recognition by various scavenger receptors on Kupffer and endothelial liver cells. J Biol Chem 266: 2282–2289

Van Velzen AG, Da Silva RP, Gordon S, Van Berkel TJC (1997) Characterization of a receptor for oxidized low-density lipoproteins on rat Kupffer cells: similarity to macrosialin. Biochem J 322: 411–415

Wang X, Greilberger J, Ledinski G, Kager G, Jurgens G (2001) Binding and uptake of differently oxidized low density lipoprotein in mouse peritoneal macrophages and THP-1 macrophages: involvement of negative charges as well as oxidation-specific epitopes. J Cell Biochem 81: 557–569

Welch KD, Davis TZ, Van Eden ME, Aust SD (2002) Deleterious iron-mediated oxidation of biomolecules. Free Radic Biol Med 32: 577–583

Wester HJ, Hamacher K, Stocklin G (1996) A comparative study of N.C.A. fluorine-18 labeling of proteins via acylation and photochemical conjugation. Nucl Med Biol 23: 365–372

Wilbur DS (1992) Radiohalogenation of proteins: an overview of radionuclides, labeling methods, and reagents for conjugate labeling. Bioconjug Chem 3: 433–470

Wuest F, Hultsch C, Bergmann R, Johannsen B, Henle T (2003) Radiolabelling of isopeptide N-epsilon-(gamma-glutamyl)-L-lysine by conjugation with N-succinimidyl-4-[^{18}F]fluorobenzoate. Appl Radiat Isot 59: 43–48

Yang C, Wang J, Krutchinsky AN, Chait BT, Morrisett JD, Smith CV (2001) Selective oxidation *in vitro* by myeloperoxidase of the N-terminal amine in apolipoprotein B-100. J Lipid Res 42: 1891–1896

Zheng G, Bachinsky DR, Stamenkovic I, Strickland DK, Brown D, Andres G, McCluskey RT (1994) Organ distribution in rats of two members of the low-density lipoprotein receptor gene family, gp330 and LRP/alpa 2MR, and the receptor-associated protein (RAP). J Histochem Cytochem 42: 531–542

Authors' address: Jens Pietzsch, PhD, Pathological Biochemistry Group, PET Center, Institute of Bioinorganic and Radiopharmaceutical Chemistry, Research Center Rossendorf, P.O. Box 51 01 19, 01314 Dresden, Germany,

Fax: 0049 351 260 3661, E-mail: j.pietzsch@fz-rossendorf.de